Antimicrobial Ambiguine Isonitriles from the Cyanobacterium *Fischerella ambigua*

Shunyan Mo, Aleksej Krunic, George Chlipala, and Jimmy Orjala*

Department of Medicinal Chemistry and Pharmacognosy, University of Illinois at Chicago, Chicago, Illinois 60612

Received November 25, 2008

Five new antibacterial ambiguine K−O isonitriles (**1**−**5**) and eight previously described indole alkaloids were isolated from the cultured cyanobacterium *Fischerella ambigua* (UTEX 1903) by bioassay-guided fractionation. The planar structures of the new compounds were determined by spectroscopic analysis including MS and 1D and 2D NMR. X-ray crystallography was used to determine the absolute stereoconfiguration of ambiguine K isonitrile. The isolates were evaluated for their antibacterial activities against a set of bacterial targets, including *Mycobacterium tuberculosis* and *Bacillus anthracis*. Ambiguine K and M isonitriles showed the most potent activity against *M. tuberculosis*, with MIC values of 6.6 and 7.5 μM, respectively. Ambiguine A isonitrile showed the most potent activity against *B. anthracis*, with a MIC of 1.0 μM.

Cyanobacteria (blue-green algae) are known to be a rich source of secondary metabolites with diverse chemical structures and biological activities.[1−6] To date, over 1000 natural products of cyanobacterial origin have been reported.[1−6] These include many biologically active compounds with anticancer, antimicrobial, antiviral, and immunosuppressive activities.[7,8] Branched filamentous cyanobacteria belonging to the order Stigonematales are known to produce antibacterial, antifungal, and antialgal isonitrile-containing indole alkaloids, such as hapalindoles,[9−14] ambiguine isonitriles,[9,15,16] fischerindoles,[17] and wetwitindolinones.[18,19] These alkaloids all have tetra- or pentacyclic carbon skeletons derived from tryptophan and geranyl diphosphate.[14,18] The ambiguine isonitriles contain an additional 1,1-dimethylallyl moiety at the 2 position of the indole ring, which often undergoes further cyclization to form the seven-membered ring observed in many ambiguine isonitriles.[20] The promising biological activities and complex chemical structures have led to several synthetic efforts toward this class of alkaloids since Moore et al. originally discovered them from cyanobacteria.[20−31]

In our preliminary studies the crude extract of *Fischerella ambigua* (Nageli) Gomont (UTEX 1903) showed significant antibacterial activity against *Mycobacterium tuberculosis* and *Bacillus anthracis*. Earlier investigations of *F. ambigua* (UTEX 1903) by Moore et al. led to the isolation of several ambiguine isonitriles and hapalindoles.[15] Initial LC-MS dereplication indicated the presence of a number of previously described ambiguine isonitriles in the extract.[32] In addition, the dereplication indicated the presence of several potentially novel ambiguine isonitriles. Bioassay-guided fractionation led to the isolation of 13 antibacterial alkaloids including five new ambiguine isonitrile derivatives as well as eight previously described indole alkaloids.

Results and Discussion

F. ambigua was mass cultured in Allen medium.[33] The freeze-dried biomass was extracted with CH_2Cl_2−MeOH (1:1) to yield a crude extract, which showed significant antibacterial activity. Five new ambiguine isonitriles (**1**−**5**) and eight previously reported alkaloids, ambiguine A−C, E, F, and I isonitriles and hapalindoles G and H, were isolated using silica gel, Sephadex LH-20, and reversed-phase chromatography. The chemical structures were identified by analysis of 1D and 2D NMR, MS, and X-ray data.

Ambiguine K isonitrile (**1**) was obtained as colorless needles (MeOH). The UV spectrum indicated the presence of an indole moiety [λ_{max} (log ϵ) 230 (2.72), 275 (2.11)]. The presence of an isonitrile moiety was evident from both ^{13}C NMR (δ 158.2) and IR (ν_{max} 2125 cm^{-1}) data. The ESI mass spectrum of **1** exhibited a 3:1 ion cluster at *m/z* 443/445 $[M + Na]^+$, indicating the presence of one chlorine atom. The HRMS gave a quasi-molecular ion $[M - H]^-$ at *m/z* 419.18979 for the molecular formula of $C_{26}H_{29}ClN_2O$. Various features of the ^{1}H (Table 1) and ^{13}C NMR (Table 2) chemical shift data suggested that **1** was an ambiguine isonitrile derivative.

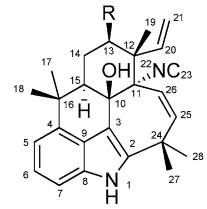

1 R = Cl
2 R = H

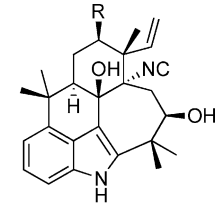

3 R = Cl
4 R = H

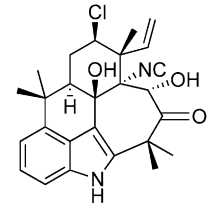

5

Analysis of the ^{1}H, COSY (Figure 1), and HSQC spectra demonstrated the presence of a 1,2,3-trisubstituted aromatic moiety with signals at δ_H 6.98 (H-5), 7.07 (H-6), and 7.09 (H-7), vinyl group signals at δ_H 6.06 (H-20), 5.43 (H-21*E*), and 5.36 (H-21*Z*), and double-bond signals at δ_H 5.73 (H-25) and 5.69 (H-26) as well as an isolated spin system consisting of three carbons: a methine at δ_H 4.47 (H-13), a methylene at δ_H 2.53 (H-14$_{ax}$) and 2.29 (H-14$_{eq}$), and a methine at δ_H 2.44 (H-15). In addition five methyl groups could be observed in the ^{1}H NMR spectrum (δ_H 1.57, H-28; 1.58, H-27; 1.62, H-19; 1.38, H-18; 1.51, H-17).

The ^{13}C NMR spectrum displayed all 26 carbon resonances implied by the molecular formula. Thirteen of these signals were observed in the region 100−160 ppm, eight of which were assigned to the indole moiety (δ_C 138.8, 111.0, 140.6, 114.2, 123.2, 108.3, 135.3, and 126.0). Another four carbons were attributed to the vinyl group (δ_C 143.2 and 118.7) and the double bond (δ_C 143.4 and 125.6), while the final deshielded resonance (δ_C 158.2) was assigned to the isonitrile moiety.[15] Of the 13 degrees of unsaturation required by the molecular formula, 10 were accounted for by the indole

* Corresponding author. Tel: 312-996-5583. Fax: 312-996-7107. E-mail: orjala@uic.edu.

10.1021/np800751j CCC: $40.75
Published on Web 04/16/2009

Table 1. ^{1}H NMR Data of Compounds **1**−**5** (900 MHz; δ_H, mult., *J* in Hz)

position	**1**[a]	**2**[b]	**3**[a]	**4**[a]	**5**[a]
5	6.98, dd (7.0, 0.8)	6.94, d (7.2)	7.00, d (7.2)	6.98, d (7.3)	7.02, dd (6.8, 1.0)
6	7.07, t (7.5)	7.04, dd (7.2, 7.8)	7.08, dd (7.2, 7.9)	7.06, dd (7.3, 7.9)	7.14, dd (6.8, 6.8)
7	7.09, dd (7.9, 0.8)	7.09, d (7.8)	7.14, d (7.9)	7.12, d (7.9)	7.13, d (6.8)
13	4.47, dd (12.5, 3.7)	1.84, t (13.3)[c] 1.52, m[d]	4.51, dd (12.6, 3.8)	2.02, ddd (14.0, 13.5, 3.4)[c] 1.55, ddd (13.5, 3.3, 3.3)[d]	4.52, dd (12.9, 3.9)
14_{ax}	2.53, ddd (13.1, 12.6, 12.5)	2.01, ddd (13.3, 13.0, 12.4)	2.55, ddd (12.6, 12.6, 12.8)	2.17, dddd (14.0, 13.0, 12.5, 3.3)	2.66, ddd (12.9, 12.9, 12.6)
14_{eq}	2.29, ddd (12.6, 3.7, 2.5)	1.77, d (12.4)	2.27, m	1.84, dddd (13.0, 3.3, 3.4, 2.4)	2.29, ddd (12.6, 3.9, 3.1)
15	2.44, dd (13.1, 2.5)	2.07, d (13.0)	2.48, dd (12.8, 2.2)	2.32, dd (12.5, 2.4)	2.37, dd (12.9, 3.1)
17	1.51, s	1.42, s	1.54, s	1.51, s	1.48, s
18	1.38, s	1.30, s	1.32, s	1.30, s	1.50, s
19	1.62, s	1.48, s	1.54, s	1.48, s	1.73, s
20	6.06, dd (17.4, 10.9)	6.11, dd (11.6, 17.6)	6.09, dd (17.4, 10.8)	6.21, dd (17.3, 11.1)	6.04, dd (17.4, 10.8)
21*E*	5.43, dd (10.9, 1.1)	5.19, br (11.6)	5.47, d (10.8)	5.26, dd (11.1, 1.6)	5.58, dd (10.8, 1.0)
21*Z*	5.36, dd (17.4, 1.1)	5.21, d (17.6)	5.34, d (17.4)	5.24, dd (17.3, 1.6)	5.45, dd (17.4, 1.0)
25	5.73, d, (12.6)	5.70, d (12.6)	3.97, dd (10.9, 1.8)	3.98, dd (10.9, 1.9)	
26	5.69, d (12.6)	5.63, d (12.6)	3.06, dd (10.9, 12.9)[c] 2.07, dd (12.9, 1.8)[d]	3.01, m[c] 2.00, dd (13.2, 1.9)[d]	4.94, s
27	1.58, s[e]	1.51, s[e]	1.29, s	1.30, s	1.62, s
28	1.57, s[e]	1.53, s[e]	1.61, s	1.61, s	1.83, s
NH		10.84, s			

[a] In MeOH-d_4. [b] In DMSO-d_6. [c] Axial. [d] Equatorial. [e] Assignments may be reversed.

Table 2. ^{13}C NMR Data of Compounds **1**−**5** (226 MHz; δ_C, mult)

position	**1** (MeOH-d_4)	**2** (DMSO-d_6)	**3** (MeOH-d_4)	**4** (MeOH-d_4)	**5** (MeOH-d_4)
2	138.8, qC	138.6, qC	139.8, qC	139.5, qC	134.2, qC
3	111.0, qC	111.3, qC	110.6, qC	111.8, qC	111.9, qC
4	140.6, qC	140.7, qC	140.1, qC	140.9, qC	140.5, qC
5	114.2, CH	113.8, CH	114.7, CH	114.5, CH	115.3, CH
6	123.2, CH	122.5, CH	123.0, CH	122.9, CH	123.7, CH
7	108.3, CH	108.1, CH	108.6, CH	108.4, CH	108.0, CH
8	135.3, qC	134.3, qC	134.9, qC	134.8, qC	135.7, qC
9	126.0, qC	125.6, qC	126.6, qC	126.7, qC	126.0, qC
10	76.5, qC	75.8, qC	75.4, qC	75.8, qC	77.8, qC
11	71.7, qC	69.7, qC	74.4, qC	73.5, qC	69.3, qC
12	50.4, qC	44.1, qC	51.4, qC	45.4, qC	50.7, qC
13	66.4, CH	35.4, CH_2	67.2, CH	37.6, CH_2	66.0, CH
14	30.2, CH_2	18.2, CH_2	30.5, CH_2	19.1, CH_2	31.0, CH_2
15	50.5, CH	49.3, CH	50.0, CH	49.7, CH	50.5, CH
16	39.0, qC	38.2, qC	38.2, qC	38.0, qC	38.9, qC
17	28.5, CH_3	29.2, CH_3	28.9, CH_3	28.9, CH_3	27.2, CH_3
18	26.5, CH_3	27.0, CH_3	26.4, CH_3	26.6, CH_3	30.3, CH_3
19	13.8, CH_3	20.7, CH_3	13.0, CH_3	19.2, CH_3	13.0, CH_3
20	143.2, CH	146.1, CH	143.6, CH	147.0, CH	143.0, CH
21	118.7, CH_2	115.4, CH_2	119.1, CH_2	115.4, CH_2	120.2, CH_2
23	158.2, qC	157.2, qC	160.2, qC	157.8, qC	[a]
24	39.8, qC	39.3, qC	41.9, qC	41.9, qC	49.5, qC
25	143.4, CH	143.1, CH	74.2, CH	74.6, CH	209.3, qC
26	125.6, CH	125.5, CH	35.4, CH_2	35.3, CH_2	85.5, CH
27	27.1, CH_3[b]	27.3, CH_3[b]	23.0, CH_3	23.4, CH_3	28.0, CH_3
28	32.1, CH_3[b]	32.4, CH_3[b]	25.5, CH_3	25.6, CH_3	32.0, CH_3

[a] Signal not observed. [b] Assignments may be reversed.

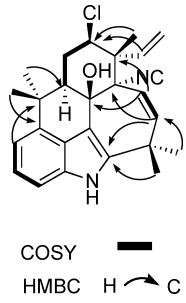

Figure 1. Key HMBC and COSY correlations of ambiguine K isonitrile (**1**).

ring, two double bonds, and the isonitrile moiety. Hence ambiguine K isonitrile was deduced to possess three additional rings.

The planar structure of ambiguine K isonitrile was established by analysis of the correlations observed in the HMBC spectrum (Figure 1). The connectivity within the indole moiety was established by the correlations from H-5 to C-9, H-6 to C-4 and C-8, and H-7 to C-9. The *gem*-dimethyl group at C-16 was connected to C-4 on the basis of the correlations observed from H_3-17 and H_3-18 to both C-4 and C-16. Further correlations from H_3-17 and H_3-18 to C-15 connected this portion to the H15−H13 COSY coupled spin system. Three-bond correlations from both H_3-19 and H-20 to C-11 and C-13 as well as from H-20 to C-12 revealed the position of the vinyl and C-19 methyl groups on C-12 and connected this fragment to C-13. In addition, correlations from H-26 to C-10, C-11, and C-12 as well as from H-25 to C-11 established a linkage of the Δ^{25} double bond to C-11. This double bond was in turn connected to C-2 of the indole via a second *gem*-dimethyl group as deduced by the correlations from H-25, H_3-27, and H_3-28 to C-2 and C-24.

Substitution with chlorine at position 13 was deduced by comparison of the chemical shift of H-13 (δ_H 4.47) and C-13 (δ_C 66.4) with those published for other ambiguine isonitriles.[15,16] Similarly, placement of the isonitrile group at C-11 (δ_C 71.7) and the hydroxyl group at C-10 (δ_C 76.5) was based upon chemical shift comparison with published data.[15,16] Although no correlations

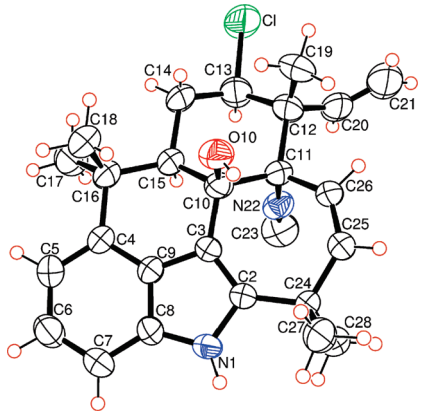

Figure 2. ORTEP diagram of ambiguine K isonitrile (**1**).

were observed to C-3 of the indole moiety in the HMBC spectrum, the connection between carbons C-10 and C-3 was established by considering the thus completed structure and the 13 degrees of unsaturation required by the molecular formula, which necessitated a pentacyclic system.

The coupling constants between H-14$_{ax}$ and H-13 (J = 12.5 Hz), as well as H-14$_{ax}$ and H-15 (J = 13.1 Hz), suggested that both H-13 and H-15 were in the axial orientation. In addition, correlations observed in the 2D NOESY spectrum between H-15 and H-13, and H-13 and H-20, indicated all to be in the same plane. This was further confirmed by the correlation observed between H-14$_{ax}$ and H$_3$-19. Together these observations established the relative configuration at positions 12, 13, and 15 as 12*R**, 13*R**, and 15*R**. The configuration of the remaining two stereocenters (positions 10 and 11) was determined by X-ray crystallography, which also confirmed the assigned structure. The absolute configuration of **1** was determined on the basis of the Flack parameter value,[34] −0.00(3), as 10*R*, 11*S*, 12*R*, 13*R*, and 15*R*. The ORTEP diagram is shown in Figure 2.

Ambiguine L isonitrile (**2**) was obtained as a white, amorphous powder. Again, the UV spectrum indicated the presence of an indole moiety [λ_{max} (log ϵ) 223 (3.47), 271 (2.91)], and the presence of an isonitrile moiety was evident from both ^{13}C NMR (δ_C 157.2) and IR (ν_{max} 2127 cm^{-1}) data. The HRMS peak at *m*/*z* 387.24347 [M + H]$^+$ suggested a molecular formula of $C_{26}H_{30}N_2O$ for **2** and the absence of chlorine in the structure. Comparison of ^{1}H and ^{13}C NMR spectra for **2** with those of **1** (Tables 1 and 2) showed that they both where closely related ambiguine isonitrile compounds. However, in the ^{1}H NMR spectrum of **2**, the resonance observed in **1** for the chlorinated methine group at δ_H 4.47 (H-13) was replaced by two signals at δ_H 1.52 (H-13$_{eq}$) and 1.84 (H-13$_{ax}$). The chlorinated C-13 methine resonance (δ_C 66.4) found in the spectrum for compound **1** was also absent in the DEPT spectrum for **2**, while an additional methylene carbon at δ_C 35.4 (C-13) was observed. These observations indicated that **2** lacked the chloro substitution at position 13 observed in **1**. This conclusion was confirmed by analysis of COSY and HSQC data, which showed the presence of a CH_2CH_2CH spin system from C-13 to C-15. On the basis of all of the above information, as well as analysis of HMBC correlations, the planar structure of **2** was established as the deschloro derivative of ambiguine K isonitrile.

The relative configuration of **2** was determined by comparison of chemical shifts and coupling constants with those of **1**, as well as correlations observed in the 2D NOESY spectrum. Similar to **1**, the coupling constant between H-14$_{ax}$ and H-15 (J = 13.0 Hz) indicated that H-15 was in the axial orientation, while the 2D NOESY correlations observed between H-13$_{ax}$, H-20, and H-15 suggested that all of these protons were in the same plane. This suggested a relative configuration of 12*R** and 15*R**. The relative configuration at C-10 (δ_C 75.8) and C-11 (δ_C 69.7) was assigned as 10*R**, 11*S** by comparison of chemical shifts with those of **1** ($\delta_{C\text{-}10}$ 76.5 and $\delta_{C\text{-}11}$ 71.7). Thus, ambiguine L isonitrile has the relative configuration of 10*R**, 11*S**, 12*R**, and 15*R**. This represents the same configuration as observed in ambiguine K isonitrile (**1**) at these positions and suggests the identical absolute configuration for ambiguine L isonitrile.

Ambiguine M isonitrile (**3**) was obtained as a white, amorphous solid. Again, the UV spectrum indicated the presence of an indole moiety [λ_{max} (log ϵ) 221 (2.64), 278 (1.92)], and the presence of an isonitrile moiety was evident from both ^{13}C NMR (δ_C 160.2) and IR (ν_{max} 2130 cm^{-1}) data. The ESI mass spectrum of **3** exhibited a 3:1 ion cluster at *m*/*z* 439/441 [M + H]$^+$, indicating the presence of a chlorine. The HRMS peak at *m*/*z* 439.2143 [M + H]$^+$ coupled with NMR information established the molecular formula as $C_{26}H_{31}ClN_2O_2$. ^{1}H and ^{13}C NMR spectra (Tables 1 and 2) of compound **3** showed signals similar to those found in ambiguine K isonitrile (**1**). The major difference was the absence of the Δ^{25} double bond, which had been replaced by a −CHCH$_2$− spin system (CH-25 and CH$_2$-26). The chemical shift of H-25 (δ_H 3.97) and C-25 (δ_C 74.2) and consideration of the molecular formula placed a hydroxyl group at C-25. The linkage of the C-25−C-26 fragment to C-11 was determined by HMBC correlations from H-25 as well as H-26$_{ax}$ and H-26$_{eq}$ to C-11. Similarly, the correlations from H-25, H$_3$-27, and H$_3$-28 to C-2 and C-24 established the connection of this moiety to C-2 of the indole via a *gem*-dimethyl group.

The relative configuration of the molecule was determined analogously to **1**. The coupling constant between H-14$_{ax}$ and H-13 (J = 12.6 Hz), as well as H-14$_{ax}$ and H-15 (J = 12.8 Hz), suggested that both H-13 and H-15 were in the axial orientation. This was confirmed by the 2D NOESY correlations observed between H-13 and both H-15 and H-20, indicating all to be in the same plane. This established the relative configuration as 12R*, 13*R**, and 15*R**. The chemical shifts of C-10 (δ_C 75.4) and C-11 (δ_C 74.4) were similar to those observed in ambiguine K isonitrile (see Table 2), indicating both compounds to have identical configuration at these positions. In addition, correlations observed in the 2D NOESY spectrum between H-26$_{ax}$, H$_3$-27, and H$_3$-19 suggested that they were in the same plane (the signals for H$_3$-19 and H$_3$-17 overlap at δ_H 1.54, but the observed correlation was assigned to H$_3$-19 due to the considerable distance between H-26$_{ax}$ and H$_3$-17). The coupling constant for H-26$_{ax}$ and H-25 (J = 10.9 Hz) indicated that H-25 was anti to H-26$_{ax}$, in agreement with the NOESY correlations observed between H-25 and H$_3$-28. Therefore, the relative configuration of C-25 was assigned as *R**, and the relative configuration of ambiguine M isonitrile (**3**) was determined as 10*R**, 11*S**, 12*R**, 13*R**, 15*R**, and 25*R**. This is the same configuration as observed in ambiguine K isonitrile (**1**) at positions 10, 11, 12, 13, and 15. The shared biosynthetic pathway for **1** and **3** suggests the absolute configuration for ambiguine M isonitrile to be 10*R*, 11*S*, 12*R*, 13*R*, 15*R*, and 25*R*.

Ambiguine N isonitrile (**4**) was obtained as a white, amorphous solid. The UV spectrum indicated the presence of an indole moiety [λ_{max} (log ϵ) 229 (3.53), 270 (3.48)], while IR (ν_{max} 2142 cm^{-1}) and ^{13}C NMR (δ_C 157.8) data showed the presence of an isonitrile moiety. The molecular formula was determined as $C_{26}H_{32}N_2O_2$ by HRMS (*m*/*z* 405.2534 [M + H]$^+$) and lacked chlorine in the structure. The ^{1}H and ^{13}C spectra (see Tables 1 and 2) for **4** indicated that it was the deschloro derivative of ambiguine M isonitrile (**3**). Comparison of ^{1}H NMR spectra showed that the signal at δ_H 4.51 (H-13) found in **3** had disappeared and was replaced by two signals at δ_H 1.55 (H-13$_{eq}$) and 2.02 (H-13$_{ax}$) in **4**. Similarly in the ^{13}C NMR spectra, the methine C-13 resonance for **3** (δ_C 67.2) had been replaced by a methylene carbon at δ_C 37.6 for **4**. COSY and HSQC data also showed the presence of a CH_2CH_2CH spin system from C-13 to C-15.

The relative configuration of **4** was determined by comparison of chemical shifts and coupling constants with those of **1** and **3**

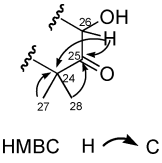

Figure 3. Structure and key HMBC correlations of the 1-hydroxy-3, 3-dimethyl-2-propanone moiety.

(Tables 1 and 2). The coupling constant between H-14_{ax} and H-15 (J = 12.5 Hz) indicated H-15 was in the axial orientation. This was confirmed by inspection of the 2D NOESY experiment, where correlations were observed between H-15, H_3-17 and H-13_{ax}, as well as between H_3-19, H-13_{eq} and H-14_{ax}, indicating H-15 and H_3-19 to be in the opposite plane. The chemical shifts of C-10 (δ_C 75.8) and C-11 (δ_C 73.5) were similar to those observed in ambiguine K isonitrile (see Table 2), indicating a 10*R**, 11*S** configuration. Similar to ambiguine M isonitrile, correlations were observed in the 2D NOESY spectrum between H-26_{ax}, H_3-19 and H_3-27, suggesting that they were in the same plane. The coupling constant for H-26_{ax} and H-25 (J = 10.9 Hz) indicated that H-25 was anti to H-26_{ax}. Thus, the relative configuration of ambiguine N isonitrile (**4**) was determined as 10*R**, 11*S**, 12*R**, 15*R**, and 25*R**. Again, this is the same configuration as observed in ambiguine K isonitrile (**1**) at positions 10, 11, 12, and 15 and suggests the absolute configuration for ambiguine N isonitrile to be 10*R*, 11*S*, 12*R*, 15*R*, and 25*R*.

Ambiguine O isonitrile (**5**) exhibited a 3:1 ion cluster at *m*/*z* 451/453 $[M - H]^-$ in the ESIMS. HRMS (*m*/*z* 451.1802 $[M - H]^-$) determined the molecular formula as $C_{26}H_{29}ClN_2O_3$. The UV spectrum indicated the presence of an indole moiety [λ_{max} (log ε) 220 (3.44), 277 (2.83)]. ^{1}H and ^{13}C NMR spectra showed signals indicative of an ambiguine isonitrile derivative (see Tables 1 and 2). The major differences as compared to ambiguine K−N isonitriles were observed in the seven-membered ring portion of the molecule. In particular, a new signal at δ_H 4.94 (H-26) appeared in the ^{1}H spectrum for compound **5** and was ascribed to a hydroxylated methine (δ_C 85.5, C-26). In addition, the ^{13}C NMR spectrum indicated the presence of a ketone moiety (δ_C 209.3, C-25). HMBC correlations from H-26 to C-24 and C-25 and from H_3-27 and H_3-28 to C-24 and C-25 suggested the presence of a 1-hydroxy-3,3-dimethyl-2-propanone moiety as part of the seven-membered ring system (Figure 3). The HMBC correlations from H-26 to C-12, C-11, and C-10 established the C-26 to C-11 connection, while the correlations from H_3-27 and H_3-28 to C-2 determined the connection of C-24 to C-2 of the indole moiety. Although no signal could be observed for the C-23 isonitrile in the ^{13}C NMR spectrum, this substituent at C-11 was determined by a characteristic IR peak (ν_{max} 2123 cm^{-1}), the molecular formula, and comparison of the chemical shift of C-11 (δ 69.3) with other ambiguine isonitrile compounds reported in this paper.

Analysis of the coupling constants and correlations in the 2D NOESY spectrum established the relative configuration of **5**. The coupling constant between H-14_{ax} and H-13 (J = 12.9 Hz), as well as H-14_{ax} and H-15 (J = 12.9 Hz), suggested that both H-13 and H-15 were axial. This was confirmed by the correlations observed in the 2D NOESY spectrum between H-13, H-15 and H_3-20, which indicated that H-13, H-15, and H-20 were all in the same plane. The chemical shifts of C-10 (δ_C 77.8) and C-11 (δ_C 69.3) were similar to those observed for ambiguine K isonitrile (see Table 2), indicating that both compounds have identical configurations at these positions. In addition, correlations observed in the 2D NOESY spectrum between H-26 and H_3-19, H-20, and H-21*Z* indicated these protons to be spatially close (integrated volumes suggested that H-26 was almost equidistant to all three protons). This required H-26 to be in pseudoequatorial position of the cycloheptene ring, and the configuration of C-26 was assigned as *S**. In this configuration, the OH group at C-26 is in pseudoequatorial position, minimizing steric interactions. In the opposite configuration (26*R**), multiple 1,3-diaxial interactions would be present, which would result in a ring twist, thus placing H-26 farther away from H_3-19. The 26*S**configuration is also supported by the lack of NOE correlation between H-26 and H_3-27 (or H_3-28). In the 26*S**configuration, the interproton distance from H-26 to H_3-27 (or H_3-28) is increased due to the flattening of the C-3−C-24−C-25 plane, similar to that observed for 3,4-benzocycloheptanone by Bodennes and St.-Jacques.[37] Thus, the relative configuration of ambiguine O isonitrile was determined as 10*R**, 11*R**, 12*R**, 13*R**, 15*R**, and 26*S**.

All isolates were evaluated for inhibition of growth of *Mycobacterium tuberculosis* and *Bacillus anthracis* as well as Vero cell toxicity. In addition, the isolates were also evaluated against a set of microorganisms, *Staphylococcus aureus*, *Mycobacterium smegmatis*, and *Candida albicans,* to determine the spectrum of activity (Table 3). Several isolates were active against *M. tuberculosis*. The most active compound was ambiguine K isonitrile (MIC 6.6 μM), while ambiguine A isonitrile showed the most potent activity against *B. anthracis* with a MIC of 1.0 μM. Most ambiguine isonitriles showed moderate toxicity in the Vero cell assay (IC_{50} ranging from 26.0 to >128 μM). Interestingly, ambiguine I isonitrile and hapalindole G displayed over 20- and 50-fold higher inhibition against *M. tuberculosis* than *B. anthracis*, respectively, with no detectable cytotoxicity in the Vero cell assay. Most of the isolates also possessed strong antifungal activities, similar to levels previously reported for other ambiguine isonitriles and hapalindoles.[16,35]

The co-occurrence of nonchlorinated and chlorinated ambiguine isonitriles in cyanobacteria of the order Stigonematales has been suggested to be due to some imperfection in the biosynthesis, and the resulting arrays of compounds have been proposed to provide an ecological advantage.[16] In our study, we observed no distinct difference in the level of antimicrobial activity of nonchlorinated versus chlorinated ambiguine isonitriles, except for *B. anthracis*, where the chlorinated ambiguine isonitriles seem to possess somewhat lower MIC values than their nonchlorinated partner (i.e., E vs I, K vs L, and M vs N).

Moore et al. have proposed that hapalindoles are biosynthesized by condensation of (*Z*)-β-ocimene and 3-((*Z*)-2′-isocyanoethenyl)indole.[10] Ambiguine isonitriles have an additional isoprene unit attached to C-2 of the indole moiety. This isoprene moiety is often cyclized to form an additional seven-membered ring. In this study we observed substantial flexibility in the degree of oxidation of this seven-membered ring portion. Ambiguine K (**1**) and L (**2**) isonitriles, both possessing a C25−C26 double bond, can be considered the precursors for ambiguine M (**3**), N (**4**), and O (**5**) isonitriles as well as the previously reported ambiguine isonitriles containing a seven-membered ring. We observed ambiguine D isonitrile only in trace amounts (detected by LC-MS, data not shown) in this study. In contrast, ambiguine D isonitrile was found to be the major ambiguine isonitrile in this strain by Moore et al.[15] We also did not observe ambiguine J isonitrile, the deschloro derivative of ambiguine D isonitrile recently found by Raveh and Carmeli[16] in a *Fischerella* sp. from Israel.

Experimental Section

General Experimental Procedures. Optical rotations were determined on a Perkin-Elmer 241 polarimeter. UV spectra were obtained on an Agilent 1100 HPLC system with a diode array detector. IR spectra were obtained on a Jasco FTIR-410 Fourier transform infrared spectrometer. ^{1}H and ^{13}C NMR spectra were obtained on a Bruker Avance DRX600 MHz NMR spectrometer with a 5 mm CPTXI Z-gradient probe and a Bruker AVII900 MHz NMR spectrometer with a 5 mm ATM CPTCI Z-gradient probe, referenced to the corresponding solvent peaks. Low-resolution ESI mass spectra were obtained on a ThermoFinnigan TSQuantum triple quadrupole mass spectrometer and an Agilent 1946A LC-MSD single quadrupole LC mass spectrometer. High-resolution ESI mass spectra were obtained on a Thermo Electron LTQ FT ICR mass spectrometer.

Table 3. MIC and IC_{50} Values of Compounds from *Fischerella ambigua* against Test Organisms *in Vitro*

compound	M. t.[a] MIC (μM)	B. a.[b] MIC (μM)	S. a.[c] MIC (μM)	M. s.[d] MIC (μM)	C. a.[e] MIC (μM)	V.[f] IC_{50} (μM)
ambiguine K isonitrile (**1**)	6.6	7.4	4.6	23.7	<0.9	53.2
ambiguine L isonitrile (**2**)	11.7	16.2	10.5	29.3	<1.0	44.6
ambiguine M isonitrile (**3**)	7.5	28.5	4.7	25.8	1.1	79.8
ambiguine N isonitrile (**4**)	27.1	30.9	5.5	48.8	<1.0	118.4
ambiguine O isonitrile (**5**)		13.8				80.7
ambiguine A isonitrile	46.7	1.0	1.8	14.8	<1.0	26.0
ambiguine B isonitrile		3.7	10.9	27.8	1.7	58.6
ambiguine C isonitrile	7.0	16.1	7.4	59.6	<1.0	78.3
ambiguine E isonitrile	21.0	3.6	1.5	1.4	<0.9	42.6
ambiguine F isonitrile	61.2					57.9
ambiguine I isonitrile	13.1	>128	8.9	59.7	1.7	>128
hapalindole G	6.8	>128	>128	34.0	>128	>128
hapalindole H	58.8	>128	>128	39.6	5.1	>128
rifampin	0.1					97.9
ciprofloxacin		0.2				
gentamicin			1.4			
moxifloxacin				0.7		
ketoconazole					0.03	

[a] *Mycobacterium tuberculosis*. [b] *Bacillus anthracis*. [c] *Staphylococcus aureus*. [d] *Mycobacterium smegmatis*. [e] *Candida albicans*. [f] Vero cells.

Biological Material. *Fischerella ambigua* was initially acquired from the Culture Collection of Algae at the University of Texas at Austin (UTEX 1903). The cyanobacterium was grown in a 2.8 L Fernbach flask containing 1 L of inorganic media (Allen media).[33] Cultures were illuminated with fluorescent lamps at 1.93 klx with an 18/6 h light/dark cycle. The temperature of the culture room was maintained at 22 °C. After 6−8 weeks, the biomass of cyanobacteria was harvested by centrifugation and then freeze-dried.

Extraction and Isolation. The freeze-dried biomass (2.14 g) from a total of 9 L of culture was extracted by repeated maceration with CH_2Cl_2−MeOH (1:1) to yield 691.1 mg of crude extract. The crude extract showed potent inhibitory activity against the TB pathogen *Mycobacterium tuberculosis* (MIC 2.7 μg/mL). A portion of crude extract (682 mg) was fractionated on silica gel using a gradient with increasing amount of MeOH in CH_2Cl_2 to afford 18 fractions. The TB-active fractions 2 (MIC 1.5 μg/mL, 247.7 mg), 7 (MIC 2.7 μg/mL, 11.5 mg), and 8 (MIC 8.3 μg/mL, 9.0 mg) were fractionated as follows. Fraction 2 was further separated using Sephadex LH-20 with MeOH as an eluent to obtain nine fractions. Fraction 2−8 (160.2 mg) was subjected to reversed-phase HPLC (Alltima C18, 10 μm, 250 × 10 mm, 4 mL/min) with a solvent gradient of MeOH−H_2O (85:15) to 100% MeOH over 20 min to afford ambiguine A isonitrile (t_R = 12.8 min, 5.8 mg), ambiguine B isonitrile (t_R = 9.8 min, 4.5 mg), ambiguine E isonitrile (t_R = 12.5 min, 13.5 mg), hapalindole H (t_R = 11.1 min, 14.0 mg), and a peak containing a mixture (t_R = 8.8 min). The mixture was further purified by RP-HPLC (Alltima C18, 10 μm, 250 × 10 mm, 4 mL/min) eluting with MeCN−H_2O (75:25) to afford **1** (t_R = 12.9 min, 2.8 mg) and **2** (t_R = 13.7 min, 2.2 mg), as well as hapalindole G (t_R = 11.2 min, 2.9 mg). Fractionation of fraction 2−7 using RP-HPLC (Alltima C18, 10 μm, 250 × 10 mm, 2 mL/min) and a solvent gradient of MeOH−H_2O (60:40) to 100% MeOH over 20 min led to two subfractions. Further chromatography of the first subfraction using RP-HPLC (Alltima C8, 5 μm, 250 × 10 mm, 3 mL/min) and a solvent gradient of MeOH−H_2O (80:20) to MeOH−H_2O (90:10) over 15 min afforded ambiguine B isonitrile (t_R = 13.2 min, 0.7 mg) and ambiguine C isonitrile (t_R = 12.7 min, 0.8 mg). The second subfraction was further fractionated using RP-HPLC (Alltima C18, 10 μm, 250 × 10 mm, 3 mL/min) and a solvent gradient of MeOH−H_2O (83:17) to MeOH−H_2O (90:10) over 20 min to give ambiguine A isonitrile (t_R = 18.6 min, 0.7 mg) and ambiguine I isonitrile (t_R = 16.7 min, 0.9 mg). The biologically active silica gel fraction 7 was fractionated using RP-HPLC (Alltima C18, 10 μm, 250 × 10 mm, 4 mL/min) and a solvent gradient of MeOH−H_2O (75:25) to 100% MeOH over 20 min to yield **3** (t_R = 14.1 min, 1.2 mg), **4** (t_R = 13.8 min, 1.0 mg), and **5** (t_R = 16.8 min, 0.4 mg). Silica gel fraction 8 was fractionated using the protocol identical to that for fraction 7 to give ambiguine F isonitrile (t_R = 14.8 min, 0.8 mg).

Ambiguine K isonitrile (1): colorless crystals (MeOH); $[\alpha]_D$ −94 (*c* 0.14, MeOH); UV (MeOH) λ_{max} (log ϵ) 230 (2.72), 275 (2.11) nm; IR (neat) ν_{max} 3416, 2965, 2125, 1631, 1452, 1377, 1323, 1086, 971, 927, 828, 755 cm^{-1}; ^1H NMR (see Table 1); ^{13}C NMR (see Table 2); HRESIMS *m/z* 419.18979 $[M - H]^-$ (calcd for $C_{26}H_{28}ClN_2O$, 419.18956).

Ambiguine L isonitrile (2): white, amorphous powder; $[\alpha]_D$ −97 (*c* 0.13, MeOH); UV (MeOH) λ_{max} (log ϵ) 223 (3.47), 271 (2.91) nm; IR (neat) ν_{max} 3734, 3410, 2961, 2127, 1568, 1454, 1320, 1082, 1022, 971, 929, 719 cm^{-1}; ^1H NMR (see Table 1); ^{13}C NMR (see Table 2); HRESIMS *m/z* 387.24347 $[M + H]^+$ (calcd for $C_{26}H_{31}N_2O$, 387.24309).

Ambiguine M isonitrile (3). white, amorphous powder; $[\alpha]_D$ −21 (*c* 0.07, MeOH); UV (MeOH) λ_{max} (log ϵ) 221 (2.64), 278 (1.92) nm; IR (neat) ν_{max} 3385, 2130, 1645, 1444, 1015, 951 cm^{-1}; ^1H NMR (see Table 1); ^{13}C NMR (see Table 2); HRESIMS *m/z* 439.21430 $[M + H]^+$ (calcd for $C_{26}H_{32}ClN_2O_2$, 439.21468).

Ambiguine N isonitrile (4): white, amorphous powder; $[\alpha]_D$ −12 (*c* 0.05, MeOH); UV (MeOH) λ_{max} (log ϵ) 229 (3.53), 270 (3.48) nm; IR (neat) ν_{max} 3735, 3367, 2928, 2142, 1684, 1652, 1540, 1510, 1456, 1081, 978, 867, 755 cm^{-1}; ^1H NMR (see Table 1); ^{13}C NMR (see Table 2); HRESIMS *m/z* 405.25340 $[M + H]^+$ (calcd for $C_{26}H_{33}N_2O_2$, 405.25365).

Ambiguine O isonitrile (5): white, amorphous powder; $[\alpha]_D$ −17 (*c* 0.03, MeOH); UV (MeOH) λ_{max} (log ϵ) 220 (3.44), 277 (2.83) nm; IR (neat) ν_{max} 3387, 2924, 2123, 1649, 1433, 1303, 1018, 950, 755 cm^{-1}; ^1H NMR (see Table 1); ^{13}C NMR (see Table 2); HRESIMS *m/z* 451.1802 $[M - H]^-$ (calcd for $C_{26}H_{29}ClN_2O_3$, 452.18667).

Ambiguine A isonitrile:[15,16] colorless crystals (MeOH and MeCN); $[\alpha]_D$ −22 (*c* 0.22, MeOH); ^1H NMR (see Table 9 in Supporting Information).

Ambiguine B isonitrile:[15,16] white, amorphous powder; $[\alpha]_D$ −11 (*c* 0.08, MeOH); ^1H NMR (see Table 9 in Supporting Information).

Ambiguine C isonitrile:[15] white, amorphous powder; $[\alpha]_D$ −6 (*c* 0.08, MeOH); ^1H NMR (see Table 9 in Supporting Information).

Ambiguine E isonitrile:[15,16] white, amorphous powder; $[\alpha]_D$ −83 (*c* 0.31, MeOH); ^1H NMR (see Table 9 in Supporting Information).

Ambiguine F isonitrile:[15,16] white, amorphous powder; ^1H NMR (see Table 9 in Supporting Information).

Ambiguine I isonitrile:[16] white, amorphous powder; $[\alpha]_D$ −106 (*c* 0.23, MeOH); ^1H NMR (see Table 9 in Supporting Information).

Hapalindole G:[15,36] white, amorphous powder; $[\alpha]_D$ −41 (*c* 0.24, MeOH); ^1H NMR (see Table 9 in Supporting Information).

Hapalindole H:[15,36] white, amorphous powder (MeOH); $[\alpha]_D$ +186 (*c* 0.22, MeOH); ^1H NMR (see Table 9 in Supporting Information).

X-ray Crystallographic Analysis of Ambiguine K Isonitrile (1).[38] Single crystals for X-ray analysis were grown from a methanol solution. A colorless crystal with dimensions 0.02 × 0.05 × 0.20 mm was used for the analysis. The diffraction data were collected on a Rigaku/MSC RAPID imaging plate area detector equipped with a normal focus sealed X-ray tube and Cu Kα radiation. Crystal data: $C_{26}H_{29}ClN_2O \cdot CH_3OH$, MW = 453.0, orthorhombic, space group *C*2 (5); a = 18.730(3) Å, b = 7.0493(11) Å, c = 20.221(3) Å, β = 110.242(9)°, V = 2505.0(9) $Å^3$; Z = 4, D_c =1.20 mg/m^3; μ = 1.54 mm^{-1}; $F000$ = 968. Total collected reflections 8507, 3626 unique reflections (R_{int} = 0.0497); final

R1 = 0.0583 for reflections with $I > 2\sigma(I)$; R1 = 0.0804, wR2 = 0.1756 for all unique data. The integration of intensities and refinement of unit cell parameters and orientation matrix were carried out using CrystalClear.[39] The WinGX package was used for completing the structure determination.[40] The structure was solved by direct methods, repeated cycling with least-squares refinement on F^2, and difference Fourier maps using SHELXL-97.[41] All non-hydrogen atoms were refined with anisotropic Gaussian displacement parameters. The Flack parameter, −0.00(3), was well-determined and used to assign the absolute configuration of the structure as C(10) *R*, C(11) *S*, C(12) *R*, C(13) *R*, and C(15) *R*.

Bacillus anthracis. The fractions and compounds were tested with concentrations from 100 μg/mL to 48.8 ng/mL using the previously described method.[42] The minimum inhibitory concentration (MIC) of each sample was calculated as the lowest concentration that prevents visible bacterial growth.

Mycobacterium tuberculosis. The inhibitory activity of fractions and compounds against *M. tuberculosis* was performed using the microplate Alamar Blue assay (MABA).[43] Virulent H37Rv strain was used in the assay. The MIC value was determined as the lowest drug concentration effecting an inhibition of ≥90%.

Other Organisms. The broth microdilution MIC method was used to test the activity of compounds against *Staphylococcus aureus*[44] and *Candida albicans*.[45]

Cytotoxicity. The cytotoxicity of compounds was evaluated using green monkey kidney cells (Vero).[46] Cell viability was measured using the CellTiter 96 aqueous nonradioactive cell proliferation assay.

Acknowledgment. We thank M. Bishop from Dr. A. Mesecar's group at UIC for performing the *B. anthracis* assay, and Dr. S. Cho, B. Wang, Y. Wang, and D. Wei from the Institute for Tuberculosis Research (ITR) at UIC for performing antibacterial, antifungal, and cytotoxicity assays. We also thank Dr. B. D. Santarsiero, Dr. Y. Wang, and Dr. C. A. Crot from the Research Resources Center (RRC) at UIC for X-ray crystallographic analysis and high-resolution mass spectrometry, respectively. The 900 MHz NMR spectrometer was funded by an NIH P41 grant (GM68944). This research was supported by an NIH grant (1R01GM0758556).

Supporting Information Available: A photomicrograph of *Fischerella ambigua* (UTEX 1903), tables with the complete NMR data of **1**−**5**, 1D NMR spectra of **1**−**5**, and ^{1}H NMR data of known compounds reported in this paper. This material is available free of charge via the Internet at http://pubs.acs.org.

References and Notes

(1) Mundt, S.; Kreitlow, S.; Nowotny, A.; Effmert, U. *Int. J. Hyg. Environ. Health* **2001**, *203*, 327–334.
(2) Kreitlow, S.; Mundt, S.; Lindequist, U. *J. Biotechnol.* **1999**, *70*, 61–63.
(3) Muller, D.; Krick, A.; Kehraus, S.; Mehner, C.; Hart, M.; Kupper, F. C.; Saxena, K.; Prinz, H.; Schwalbe, H.; Janning, P.; Waldmann, H.; Konig, G. M. *J. Med. Chem.* **2006**, *49*, 4871–4878.
(4) Luesch, H.; Pangilinan, R.; Yoshida, W. Y.; Moore, R. E.; Paul, V. J. *J. Nat. Prod.* **2001**, *64*, 304–307.
(5) Singh, S.; Kate, B. N.; Banerjee, U. C. *Crit. Rev. Biotechnol.* **2005**, *25*, 73–95.
(6) Jaiswal, P.; Singh, P.; Prasanna, R. *Can. J. Microbiol.* **2008**, *54*, 701–717.
(7) Sielaff, H.; Christiansen, G.; Schwecke, T. *IDrugs* **2006**, *9*, 119–127.
(8) Tan, L. T. *Phytochemistry* **2007**, *68*, 954–979.
(9) Huber, U.; Moore, R. E.; Patterson, G. M. L. *J. Nat. Prod.* **1998**, *61*, 1304–1306.
(10) Moore, R. E.; Cheuk, C.; Yang, X. Q. G.; Patterson, G. M. L.; Bonjouklian, R.; Smitka, T. A.; Mynderse, J. S.; Foster, R. S.; Jones, N. D. *J. Org. Chem.* **1987**, *52*, 1036–1043.
(11) Klein, D.; Daloze, D.; Braekman, J. C.; Hoffmann, L.; Demoulin, V. *J. Nat. Prod.* **1995**, *58*, 1781–1785.
(12) Doan, N. T.; Stewart, P. R.; Smith, G. D. *FEMS Microbiol. Lett.* **2001**, *196*, 135–139.
(13) Moore, R. E.; Yang, X.-Q. G.; Patterson, G. M. L.; Bonjouklian, R.; Smitka, T. A. *Phytochemistry* **1989**, *28*, 1565–1567.
(14) Moore, R. E.; Cheuk, C.; Patterson, G. M. L. *J. Am. Chem. Soc.* **1984**, *106*, 6456–6457.
(15) Smitka, T. A.; Bonjouklian, R.; Doolin, L.; Jones, N. D.; Deeter, J. B.; Yoshida, W. Y.; Prinsep, M. R.; Moore, R. E.; Patterson, G. M. L. *J. Org. Chem.* **1992**, *57*, 857–861.
(16) Raveh, A.; Carmeli, S. *J. Nat. Prod.* **2007**, *70*, 196–201.
(17) Park, A.; Moore, R. E.; Patterson, G. M. L. *Tetrahedron Lett.* **1992**, *33*, 3257–3260.
(18) Stratmann, K.; Moore, R. E.; Bonjouklian, R.; Deeter, J. B.; Patterson, G. M. L.; Shaffer, S.; Smith, C. D.; Smitka, T. A. *J. Am. Chem. Soc.* **1994**, *116*, 9935–9942.
(19) Jimenez, J. I.; Huber, U.; Moore, R. E.; Patterson, G. M. L. *J. Nat. Prod.* **1999**, *62*, 569–572.
(20) Richter, J. M.; Ishihara, Y.; Masuda, T.; Whitefield, B. W.; Llamas, T.; Pohjakallio, A.; Baran, P. S. *J. Am. Chem. Soc.* **2008**, *130*, 17938–17954.
(21) Muratake, H.; Natsume, M. *Tetrahedron* **1990**, *46*, 6331–6342.
(22) Muratake, H.; Natsume, M. *Tetrahedron* **1990**, *46*, 6343–6350.
(23) Muratake, H.; Kumagami, H.; Natsume, M. *Tetrahedron* **1990**, *46*, 6351–6360.
(24) Fukuyama, T.; Chen, X. *J. Am. Chem. Soc.* **1994**, *116*, 3125–3126.
(25) Baran, P. S.; Richter, J. M. *J. Am. Chem. Soc.* **2005**, *127*, 15394–15396.
(26) Baran, P. S.; Richter, J. M. *J. Am. Chem. Soc.* **2004**, *126*, 7450–7451.
(27) Reisman, S. E.; Ready, J. M.; Hasuoka, A.; Smith, C. J.; Wood, J. L. *J. Am. Chem. Soc.* **2006**, *128*, 1448–1449.
(28) Baran, P. S.; Maimone, T. J.; Richter, J. M. *Nature (London)* **2007**, *446*, 404–408.
(29) Kinsman, A. C.; Kerr, M. A. *Org. Lett.* **2001**, *3*, 3189–3191.
(30) Vaillancourt, V.; Albizati, K. F. *J. Am. Chem. Soc.* **1993**, *115*, 3499–3502.
(31) Chandra, A.; Viswanathan, R.; Johnston, J. N. *Org. Lett.* **2007**, *9*, 5027–5029.
(32) Lin, Y.; Schiavo, S.; Orjala, J.; Vouros, P.; Kautz, R. *Anal. Chem.* **2008**, *80*, 8045–8054.
(33) Anderson, R. A.; Berges, J. A.; Harrison, R. J.; Watanabe, M. M. In *Algal Culturing Techniques*; Anderson, R. A., Ed.; Elsevier Academic Press: Burlington, MA, 2005; pp 429−538.
(34) Flack, H. D. *Acta Crystallogr. Sect. A* **1983**, *A39*, 876–881.
(35) Ravi, K. A.; Arunima, S.; Akhilesh, P. S.; Deepali, Sureshwar, P. S.; Gopal, N.; Ranjana, S.; Brahm, S. S. *J. Appl. Phycol.* **2006**, *18*, 33–39.
(36) Moore, R. E.; Cheuk, C.; Yang, X. Q. G.; Patterson, G. M. L.; Bonjouklian, R.; Smitka, T. A.; Mynderse, J. S.; Foster, R. S.; Jones, N. D. *J. Org. Chem.* **1987**, *52*, 1036–1043.
(37) Bodennec, G.; St.-Jacques, M. *Can. J. Chem.* **1976**, *55*, 1199–1206.
(38) Crystallographic data for the structure(s) reported in this paper have been deposited with the Cambridge Crystallographic Data Centre under deposition number CCDC 716191. Copies of the data can be obtained, free of charge, on application to the Director, CCDC, 12 Union Road, Cambridge CB2 1EZ, UK (fax: +44-(0)1223-336033 or e-mail: deposit@ccdc.cam.ac.uk).
(39) *CrystalClear, Version 1.3.6*; Rigaku Corporation: Tokyo, Japan, 1999.
(40) Farrugia, L. J. *J. Appl. Crystallogr.* **1999**, *32*, 837–838.
(41) *SHELXTL, Version 5.1*; Bruker Analytical X-ray Systems: Madison, WI, 1998.
(42) Athamna, A.; Athamna, M.; Abu-Rashed, N.; Medlej, B.; Bast, D. J.; Rubinstein, E. *J. Antimicrob. Chemother.* **2004**, *54*, 424–428.
(43) Collins, L.; Franzblau, S. G. *Antimicrob. Agents Chemother.* **1997**, *41*, 1004–1009.
(44) Isenberg, H. D., *Clinical Microbiology Procedures Handbook*; American Society for Microbiology: Washington D.C., 2002; Vol. 1, pp 1−29.
(45) Clinical and Laboratory Standards Institute. *Reference method for broth dilution antifungal susceptibility testing of filamentous fungi. Approved standard*; NCCLS document M38-A, Wayne, PA, 2002.
(46) Cantrell, C. L.; Lu, T.; Fronczek, F. R.; Fischer, N. H.; Adams, L. B.; Franzblau, S. G. *J. Nat. Prod.* **1996**, *59*, 1131–1136.

NP800751J